Electrochimica Acta 178 (2015) 608–616

Contents lists available at ScienceDirect

Electrochimica Acta

journal homepage: www.elsevier.com/locate/electacta

Biopolymer Stabilized Nanogold Particles on Carbon Nanotube Support as Sensing Platform for Electrochemical Detection of 5-Fluorouracil *in-vitro*

M. Satyanarayana, K.Yugender Goud, K.Koteshwara Reddy, K.Vengatajalabathy Gobi*

Department of Chemistry, National Institute of Technology, Warangal, Telangana 506004, India

ARTICLE INFO

Article history:
Received 11 May 2015
Received in revised form 24 July 2015
Accepted 10 August 2015
Available online 12 August 2015

Keywords:
5-Fluorouracil
Carbon nanotubes
Gold Nanoparticles
Chitosan
Electrocatalysis
Voltammetric determination

ABSTRACT

A fast and facile electrochemical sensor for the detection of an important anti-cancer drug, 5-fluorouracil, is fabricated using a gold nanoparticle decorated multiwall carbon nanotube (GNP-MWCNT) composite modified electrode. GNP-MWCNT composite has been prepared by a simple one-pot synthesis in the presence of chitosan, which acts as a reducing as well as stabilizing agent. Synthesized GNP-MWCNT is characterized by UV-Visible spectroscopy, Raman spectroscopy, XRD analysis and FESEM for the structural and chemical properties of nanocomposite, and the size of the gold nanoparticles is determined to be ~30 nm by different methods. The electrochemical capability of the fabricated GNP-MWCNT composite modified electrode for the detection of 5-FU is examined by cyclic voltammetry, electrochemical impedance analysis and differential pulse voltammetry. The nanoAu decorated carbon nanotube electrode is found to be efficient for electrocatalytic oxidation of 5-FU. Peak current of the DPVs exhibited a linear relationship against 5-FU over a wide concentration range of 0.03–10 μM with a low-detection-limit ($3\sigma/b$) of 20 nM, and the analysis time is as low as 25 s. Practical utility of the developed GNP-MWCNT nanocomposite biosensor has been demonstrated for the detection of 5-FU directly from artificial urine and pharmaceutical formulations with good recovery limits.

1. Introduction

In recent years, various antitumor active compounds are widely used in the treatment of cancer, and one of the most widely used drugs for chemotherapy of solid tumors is 5-fluorouracil (5-FU). It is an antineoplastic agent used for the treatment of solid tumor based cancers. Generally, high serum concentrations of drugs are necessitated to effect a pharmacological activity against tumors, but 5-FU metabolizes rapidly in the body. Determining safe and effective dosage of drugs for chemotherapy is still a substantial challenge in the treatment of neoplastic diseases. Frequent measurement of the concentration of 5-FU in physiological fluids is extremely demanded to maintain an optimal concentration of 5-FU. It is noteworthy that an overdose of 5-FU may cause very high toxicity by accumulation in cancer patients. Controlling the amount of 5-FU in a given formulation and the dose to the sufferers is important in pharmaceutical quality control and for clinical diagnosis. Various analytical methods have been aimed for the detection of 5-FU based on spectroscopic [1,2], chromatographic capillary [3,4], electrophoresis [5] and electrochemical methods [6–8]. Electrochemical transduction methodologies are advantageous because they offer miniaturization, portable analysis, rugged instrumentation with no movable parts, high sensitivity, on-site analysis, etc. However, the major problem towards the detection of 5-FU by an electrochemical method is the poor oxidation of 5-FU at bare electrodes and only a few electrochemical sensors have been reported so far for the detection of 5-FU. Therefore, highly sensitive and selective sensor systems are still in need for the determination of 5-FU at nano molar levels.

Carbon nanotubes (CNTs) are investigated immensely in a wide variety of research fields because of their salient features, such as high mechanical strength, nanowires of few hundred micrometer long tubular geometry and chemically inert nature with high electrical conductivity [9,10]. However, low dispersion and high aggregation impediment the effective usage of CNTs for electrochemical sensor applications. Incorporation of functional reactive groups into the backbone of CNTs and combined use with ionic liquids, polymer electrolytes, etc. could alleviate the drawbacks. In electrochemical sensor systems, CNT based electrodes are less susceptible to electrode fouling and thus the reuse of such sensors would be greatly improved [11,12].

* Corresponding author. Correspondance: Dr. K. V. GOBI, Associate Professor, Department of Chemistry, National Institute of Technology, Warangal, Telangana 506 004, INDIA. E-mail: drkvgobi@gmail.com (K.V. Gobi) Tel.:+ +91 870 2462674.

http://dx.doi.org/10.1016/j.electacta.2015.08.036
0013-4686/

Another interesting nanomaterial for the modification of electrode surface is gold nanoparticles (GNPs), because of the high surface area along with high conductivity. GNPs allow electrons to flow freely into the material and have demonstrated high catalytic activity for both oxidation and reduction reactions. The major problem with the nanoparticles is aggregation of particles, which could lead to the decrease of both active surface area and also conductivity. Therefore, it is necessary to develop effective methods to synthesize gold nanoparticles which could be free from aggregation. Several strategies have been developed to prevent the nanoparticles from aggregation such as polymer coatings, surfactant stabilizers, thiol-ligand coatings and polymer agents capping [13–15]. Considering the advantages of both MWCNTs and GNPs towards electrode modification, a hybrid composite between MWCNTs and GNPs is intended to avoid aggregation and also to bring some special features by synergistic effect.

Chitosan (chit) obtained by partial deacetylation of the natural biopolymer, chitin, is used here to form a linkage between MWCNTs and GNPs. Chitosan polymer has attracted here for the dispersion of CNTs because of the presence of a large number of functional groups such as hydroxyl and amine groups in addition to its very good film forming ability, hydrophilicity and biocompatibility. In our previous work, we fabricated a MWCNT-chitosan nanocomposite based electrode which exhibited an excellent catalytic activity, and there chitosan formed a very good linkage between MWCNT and electrode substrate [16]. In this investigation, MWCNT decorated with GNPs is synthesized in the presence of chitosan. The functional groups present in chitosan are responsible for both the reduction and stabilization of the GNPs with which the nanoparticles become stable and free from aggregation. Chitosan can also be chosen to avoid the use of toxic reductants such as hydrazine and sodium borohydride. By combining these advantages of chitosan, we fabricated an electrochemical sensor for the important anti-cancer drug 5-flourouracil using a nanocomposite of MWCNT and GNPs.

2. Experimental:

2.1. Chemicals

5-Fluorouracil, ascorbic acid, uric acid, dopamine and serotonin were obtained from Tokyo chemical industry, Japan. Chitosan (60–120 kDa, 85% deacetylation) and gold (III) chloride ($HAuCl_4$) were purchased from Sigma Aldrich, USA. MWCNTs (95%, 20–30 nm OD and 10–30 μm length) were purchased from Sisco research laboratories, India. Other chemicals used in this investigation were analytical grade reagents (minimum 99% purity). Britton-Robinson buffer (B-R buffer) was prepared by mixing boric acid, phosphoric acid and acetic acid 40 mM each, followed by the addition of 0.1 M NaOH to adjust the pH (pH 4.0 to 11.0). Artificial urine solution was prepared following a procedure reported in the literature [17]. It consists urea (170 mM), citric acid (2.0 mM), lactic acid (1.1 mM), sodium chloride (90 mM), ammonium chloride (25 mM), sodium sulphate (10 mM), sodium bicarbonate (25 mM), calcium chloride (2.5 mM), potassium dihydrogen phosphate (7.0 mM) and dipotassium hydrogen phosphate (7.0 mM), and the solution was adjusted to pH 8.0 by the addition of 1.0 M NaOH. Double distilled water filtered finally through a 0.2 μm Millipore cartridge was used to prepare aqueous solutions throughout the experiment.

2.2. Methods

2.2.1. Functionalization of MWCNTs

Functionalization of MWCNT with carboxyl groups was carried out by treating with hot nitric acid, following a procedure reported in the literature [18]. MWCNT (120 mg) was taken in 10 mL of 3 M nitric acid and heated at 60 °C for one day. Then, the black solid product was filtered, washed with water until the filtrate becomes neutral and dried at 80 °C for one day. On treatment with nitric acid, MWCNT is introduced with carboxyl groups at the sidewall defects and at the ends of the nanotubes. The resultant functionalized MWCNT was characterized by Raman spectroscopy. The number of carboxyl groups present in the functionalized MWCNT was determined by acid-base titration method, and it is 2.1 mmol g^{-1}.

2.2.2. Synthesis of GNP-MWCNT nanocomposite

The nanocomposite of GNP and MWCNT was prepared by adopting major changes in the recipe reported previously for GNP [19]. A solution of chitosan (1% w/v) was prepared by dissolving it in aqueous acetic acid (1% v/v). MWCNT (5 mg) was added to 10 mL of the chitosan solution and ultrasonicated until a homogeneous black suspension was obtained. Then, 5 mL of aq. 10 mM $HAuCl_4$ was added to the resultant MWCNT–chitosan mixture and heated for 1 h at ~80 °C. Wine red coloured gold nanoparticles can be observed in the black suspension which are protected by chitosan biopolymer. The homogeneous mixture was then stirred for 1 h to allow the chitosan protected GNPs to attach with MWCNTs through the functional —COOH groups of MWCNT and the amine groups of protecting chitosan layer. The GNP-attached MWCNTs are collected by centrifugation of the above mixture, and the GNPs which are not attached to MWCNTs and remaining in the supernatant are discarded. The collected solid product is denoted hereafter as GNP-MWCNT nanocomposite.

2.2.3. Fabrication of modified electrodes

Glassy carbon electrodes of 3 mm diameter (CH Instruments, USA) were polished with alumina powder of 1 μm size and down to 50 nm and washed well under ultrasonication with water, aq. 1:1 nitric acid, ethanol and finally with water. GNP-MWCNT nanocomposite or MWCNT (3 mg) was dispersed into a solution of chitosan (1% w/v, 1 mL) under ultrasonication at RT for about 30 min. The resultant dispersions of GNP-MWCNT and MWCNT (10 μL) were used to form a thin film on the GCE surface by drop-casting method. The resultant electrodes were dried at RT for 24 h and denoted hereafter as GNP-MWCNT-Chit/GCE and MWCNT-Chit/GCE.

2.3. Characterization

UV-Visible spectra were recorded on PerkinElmer LAMBDA25 spectrophotometer. Raman spectra of MWCNT samples were recorded using a confocal spectrometer (Model: LabRAM, HR800). A He-Ne laser source (633 nm; 20 mW power) was used for excitation, and the data were collected for 10 s using a 5× objective. Powder X-ray diffraction (XRD) of GNP-MWCNT composite was recorded in the range of 10°–90° 2θ on a Brucker AXS D8 diffractometer, and Cu was used as the target (K = 1.5406 Å) with a step size of 0.002° and a scan speed of 0.5 s per step. Surface morphological studies were carried out on an FEI Quanta 200F field emission scanning electron microscope (FESEM) operating at 15 kV. For FESEM analysis, the samples were cast on a conducting carbon tape and sputtered with a thin layer of gold to avoid charging during the analysis.

2.4. Electrochemical analysis

Voltammetry experiments were carried out using an Electrochemical Potentiostat/Galvanostat (Model 619d, CH Instruments, USA). Electrochemical impedance measurements were carried out using an electrochemical workstation (Model: IM6e, Zahner, Germany) equipped with Thales software. A conventional two-

compartment three-electrode cell of 20 mL volume was used with bare or modified GCE as the working electrode, spiral Pt electrode as the counter electrode and Ag|AgCl (3 N KCl) as reference electrode. Electrode potentials were referred against Ag|AgCl (3 N KCl) throughout the manuscript. B-R buffer (pH 4.0–11.0) was used as the electrolyte for electrochemical experiments. For electrochemical analysis, the experimental solutions were purged with nitrogen gas for 10 min prior to the start of the experiment.

3. Results and Discussion

3.1. Characterization of GNP-MWCNT nanocomposite

Formation of gold nanoparticles is usually first examined by UV–Visible spectra of the colloidal gold solution. UV-Visible spectra of the colloidal solution of chitosan protected GNPs, chitosan solution and aq. $HAuCl_4$ solution were recorded. The absorption maxima (λ_{max}) of the GNP colloidal solution is observed at 525 nm (Fig. 1A), which indicates that the size of gold nanoparticles is about ~30 nm in diameter [20,21].

XRD was used to further confirm the size of GNP in the GNP-MWCNT composite. The powder XRD patterns of MWCNT and GNP-MWCNT are shown in Fig. 1B. XRD pattern of GNP-MWCNT has all Bragg's reflections associated to crystalline gold, which were observed at 38.2°, 44.4°, 64.6°, 77.5° and 81.8°, representing (1 1 1), (2 0 0), (2 2 0), (3 1 1) and (2 2 2) planes of FCC crystalline gold (JCPDS No. 04 - 0784). The crystalline size of GNP was calculated using Scherrer formula, and the average crystalline size obtained from the calculation is ~28.7 nm. The results clearly indicate that the GNPs are of finite size and that the aggregation of nanoparticles is well controlled.

Raman spectroscopy is an important and powerful technique for characterization of CNTs and other nanomaterials [22,23]. Structural changes caused by the functionalization of MWCNT and by the decoration with GNPs can be observed by changes in Raman spectroscopy bands. Fig. 1C shows the Raman spectra recorded for pristine MWCNT, functionalized MWCNT and GNP-decorated MWCNT, where all the three samples are exhibiting D-band (~1,330 cm^{-1}) related to structural disorders of carbon based materials, G-band (~1,580 cm^{-1}) related to graphitized carbon and G^1-band (~2,660 cm^{-1}) is the first overtone of the D-band. The intensity ratio (I_D/I_G) is an indicator of the quantitative measure of structural defects. Functionalization of MWCNTs is evident from the I_D/I_G peak intensity ratio, where we observed a remarkable increase in I_D/I_G value from pristine (1.18) to functionalized MWCNT (1.46). This observation clearly confirms that the graphitized carbon content relatively decreased in functionalized MWCNT obviously owing to the functionalization process, which involves in the formation of carboxyl groups at the defect sites and at the end of the nanotubes. Further, the decoration with GNPs on functionalized MWCNT is confirmed by the peak position and intensities of D, G, and G^1 bands. At first, there was no significant difference in the I_D/I_G ratio between GNP-MWCNT and functionalized MWCNT. It indicates that the decoration of GNPs onto the surface of functionalized MWCNTs did not affect the core CNT structure. However, there is a little shift in the G-band to higher wavenumber by GNP decoration onto MWCNT (Fig. 1C inset), and it indicates the chemical interaction between GNPs and the functionalized MWCNT. A similar trend is also observed with the G^1 band.

The field emission scanning electron microscope (FESEM) was used to characterize the surface morphology of GNP-MWCNT

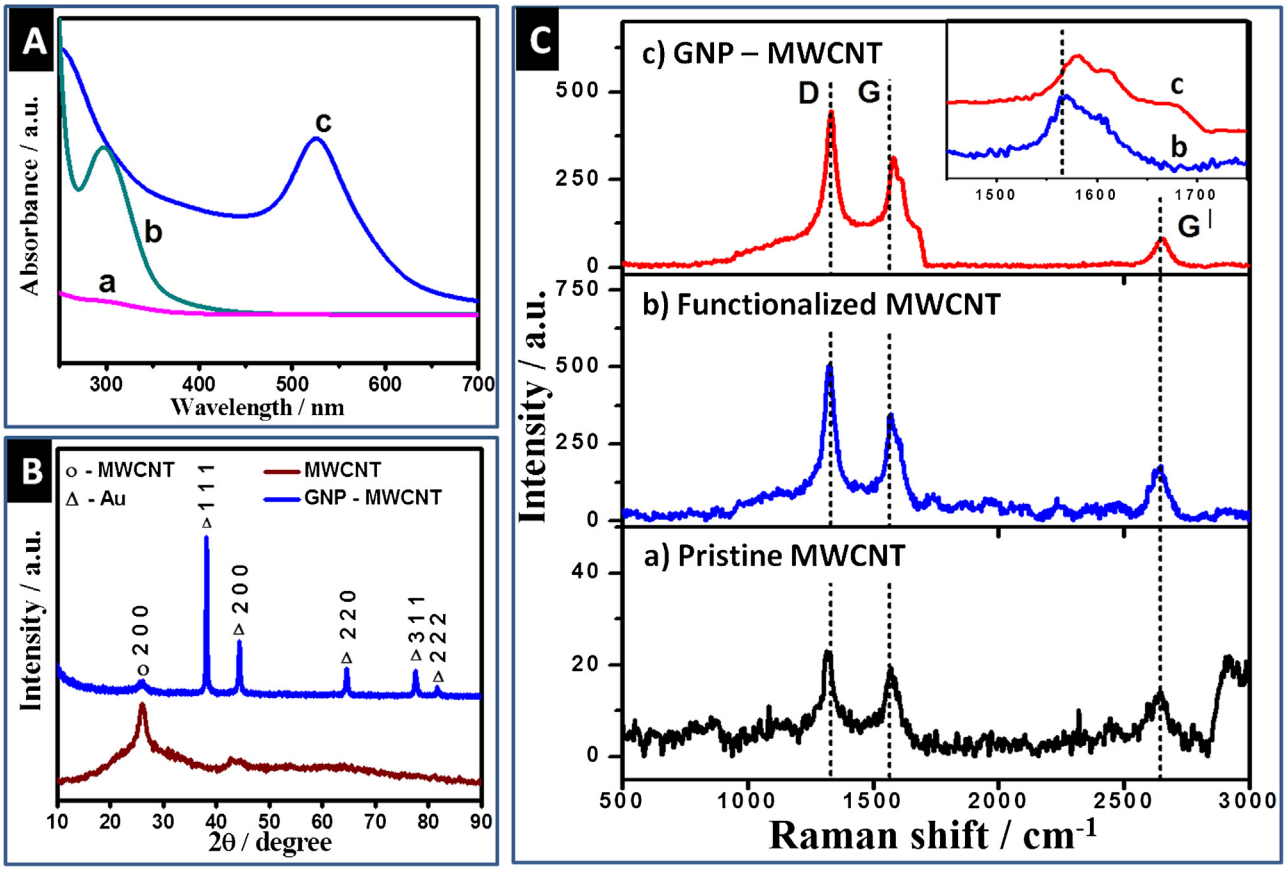

Fig. 1. (A) UV-Visible spectra of a) aq. 1 wt.% chitosan, b) aq. $HAuCl_4$, c) gold colloid in aq. 1 wt.% chitosan. (B) XRD spectra of MWCNT and GNP-MWCNT composite. (C) Raman spectra of pristine MWCNT, functionalized MWCNT and GNP-MWCNT.

nanocomposite. Fig. 2 shows the FESEM images of MWCNT and GNP-MWCNT nanocomposite. The FESEM image of GNP-MWCNT composite is seen to have sharp crystallites continuously throughout the CNT structure. Obviously, the FESEM image of plain MWCNT shows simple thread like structures of MWCNT. Fig. 2 clearly illustrates that the gold nanoparticles are distributed all over the surface of MWCNT as sharp crystallites and have formed a good network on MWCNT. Furthermore, the GNP-MWCNT film is of very much porous nature with a fine distribution of MWCNTs all over the matrix, and in overall the nanocomposite could promote the electron transfer across the film efficiently.

3.2. Electrocatalytic oxidation of 5-fluorouracil

The cyclic voltammetry analysis is a very basic method to analyze electrochemical characteristics of an analyte at modified electrodes. At first, the electroactive areas of the modified electrodes were estimated by cyclic voltammetry and compared with that of bare GCE. For the purpose, cyclic voltammograms (CVs) of $K_3[Fe(CN)_6]$ were recorded at bare GCE, MWCNT-Chit/GCE and GNP-MWCNT-Chit/GCE electrodes in aq. 2 mM $K_3[Fe(CN)_6]$ + 0.1 M KCl at various scan rates (10 to 150 mV s^{-1}). CVs recorded at the scan rate of 100 mV s^{-1} and the plot of peak currents against the square root of scan rate are shown in supplementary (Fig. S1). The peak currents observed with the modified electrodes are higher than that observed with bare GCE. The results were analyzed, and the effective surface areas of the modified electrodes were determined by applying the Randles-Sevicik equation and by considering the diffusion coefficient of $K_3[Fe(CN)_6]$ as 6.7×10^{-6} cm^{-2} s^{-1}, according to the procedure recorded elsewhere [24]. The effective surface area of bare GCE is 0.078 cm^2, which is nearly equal to the geometrical surface area of 3 mm diameter electrode. The electroactive surface areas of MWCNT-Chit/GCE and GNP-MWCNT-Chit/GCE are nearly 4 to 7 times higher than that of bare GCE and are 0.26 and 0.58 cm^2, respectively.

Cyclic voltammograms of 5-fluorouracil were recorded at bare GCE, MWCNT-Chit/GCE and GNP-MWCNT-Chit/GCE in B-R buffer (pH 8.0) containing 0.5 mM 5-FU, and the CVs are shown in Fig. 3. In the absence of 5-FU, no characteristic peak was observed at any of the electrodes in B-R buffer. In the presence of 5-fluorouracil, an irreversible anodic peak was observed at all the electrodes. The anodic peak potential for the oxidation of 5-FU at bare GCE is ~+1.25 V. At both MWCNT-Chit/GCE and GNP-MWCNT-Chit/GCE electrodes, a well-defined anodic peak was observed at a less positive potential, +1.10 V. The decrease in the overpotential for the oxidation of 5-FU at GNP-MWCNT-Chit/GCE is advantageous.

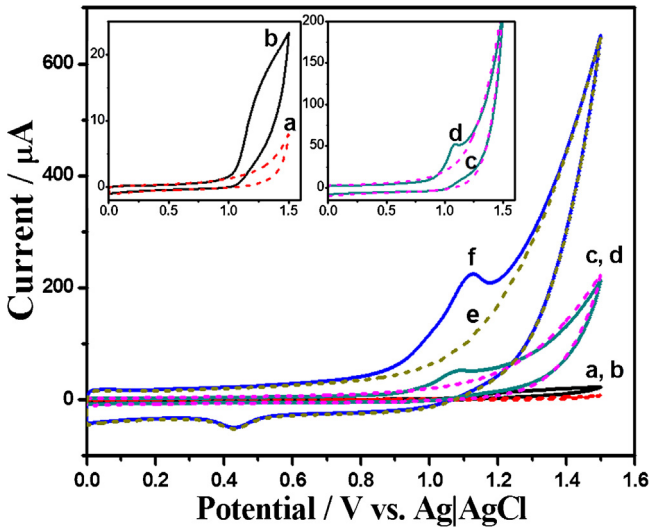

Fig. 3. CVs recorded at bare GCE (a, b), MWCNT-Chit/GCE (c, d) and GNP-MWCNT-Chit/GCE (e, f) in the presence (b, d, f) and absence (a, c, e) of 0.5 mM 5-FU in B-R buffer (pH 8.0). Scan rate: 100 mV s^{-1}.

Furthermore, the peak currents for the oxidation of 5-FU at GNP-MWCNT-Chit/GCE and MWCNT-Chit/GCE electrodes are respectively higher by 4 and 15 times than that at bare GCE. These observations are clear evidences for the enhanced effect of GNP-MWCNT nanocomposite towards 5-FU oxidation. Moreover, the GNP-MWCNT modified electrode shows a large background charging current compared with MWCNT-Chit/GCE and bare GCE, owing to a significant increase in the active surface area of the electrode. These results clearly reveal that the GNP-MWCNT nanocomposite film formed a better electron conduction pathway for the oxidation of 5-FU and helped to accelerate the electron transfer across the electrode interface.

Effect of pH on the electrochemical characteristics of 5-FU was investigated at GNP-MWCNT-Chit/GCE in B-R buffer of different pH values (pH 4.0 to 11.0) by cyclic voltammetry (Fig. 4). The pH of the buffer solution obviously influenced the oxidation peak of 5-FU. The peak currents are high in the pH range of 7.0–9.0, and it decreased to a minimum at pH ≥ 10.0. The peak potential (Ep) was gradually changing to less positive potentials as the pH varied from 5.0 to 11.0. The plot between Ep and pH (Fig. 4B) shows that Ep is linearly dependent on pH (Fig. 4B). The slope of the Ep vs. pH plot is 0.062 V and is very close to the theoretical Nernstian value of 0.059 V, which indicates that the number of protons and the

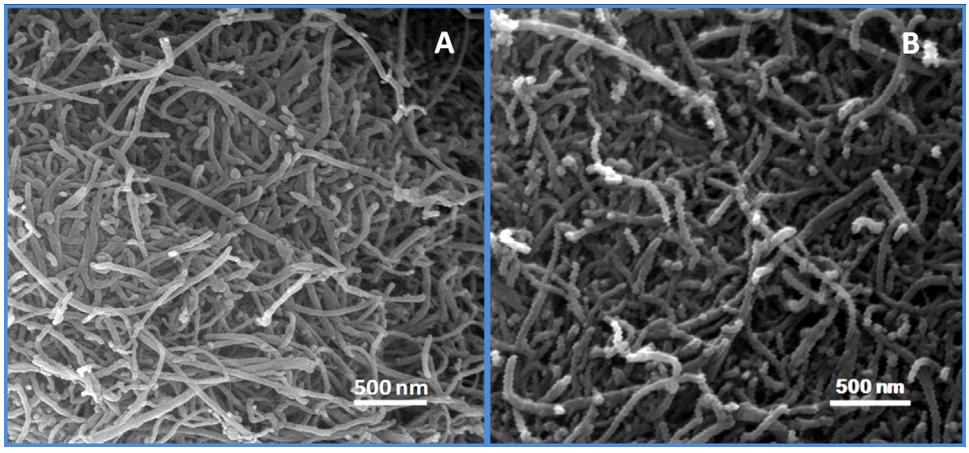

Fig. 2. FESEM images of MWCNT and GNP-MWCNT nanocomposite.

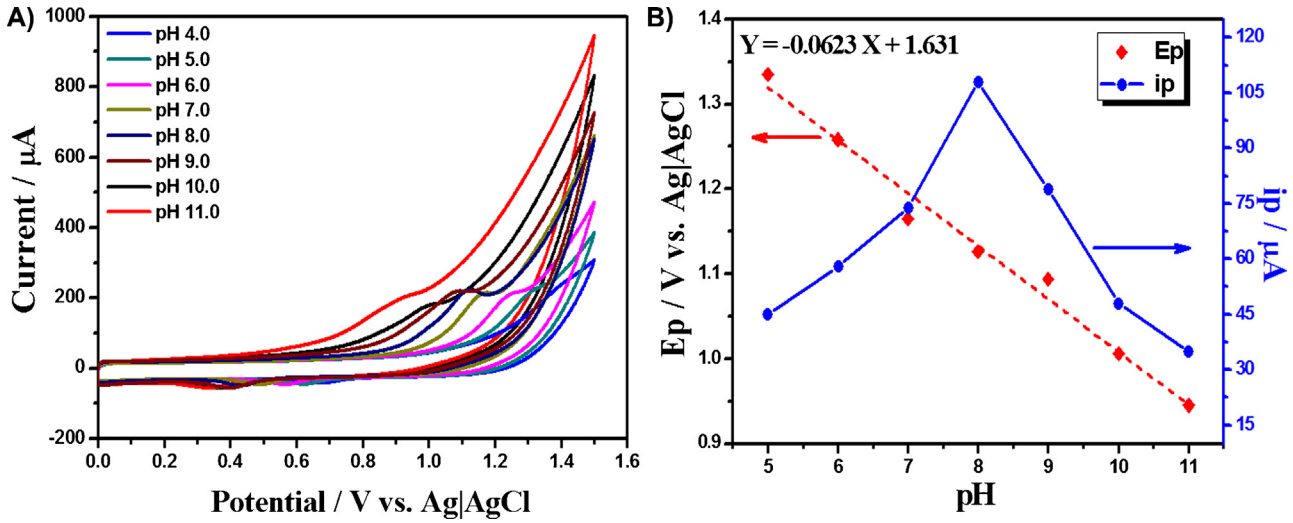

Fig. 4. (A) CVs recorded at GNP-MWCNT-Chit/GCE in the presence of 0.5 mM 5-FU in B-R buffer of different pH values (4.0–11.0). Scan rate: 100 mV s^{-1}. (B) Plots of Ep vs. pH and i_p vs. pH.

number of electrons transferred in the electrochemical oxidation of 5-FU are equal to each other. In the overall pH range of 4.0 to 11.0, the peak current was very high at pH 8.0. Considering these observations, B-R buffer of pH 8.0 has been chosen for further analysis.

Influence of the scan rate on the voltammetric behavior of 5-FU was studied. Cyclic voltammograms of 0.5 mM 5-FU at GNP-MWCNT-Chit/GCE were recorded with different scan rates (20–350 mV s^{-1}) and are shown in Fig. 5. The peak currents for oxidation of 5-FU gradually increased with the scan rate. The plot between the anodic peak current and the square root of scan rate was linear, passing through the origin (Fig. 5(B)). It clearly indicates that the electrochemical oxidation of 5-FU is a diffusion controlled process and that the permeation of 5-FU across the GNP nanocomposite film is very facile (*vide infra*).

For an irreversible electrochemical reaction, the relationship between the peak potential Ep and the scan rate ν is expressed in Eq. (1) by Laviron [25]:

$$Ep = E^{\circ} + \frac{RT}{\alpha nF} In \left[\frac{RTk^{\circ}}{\alpha nF}\right] + \left[\frac{RT}{\alpha nF}\right] ln(\nu) \quad (1)$$

where α is the charge transfer coefficient, k° is the standard rate constant for the heterogeneous electron transfer, n is the number of electrons involved in the reaction and E° is the formal potential. According to Eq. (1), the αn value can be determined from the slope of Ep vs. ln(ν) plot (Fig. S2(A), supplementary information), and k° can be calculated from the intercept of the plot if the value of E° is known. The value of E° can be obtained from the intercept of the Ep vs. ν plot (Fig. S2(B), supplementary information) by extrapolation to the vertical axis at $\nu = 0$ and is 1.08 V. From the slope of the Ep vs. ln(ν) plot, αn was calculated to be 0.56. Generally, α can be assumed to be 0.5 for an irreversible electrode process. So the electron transfer number (n) for the electrochemical oxidation of 5-FU becomes 1, and the k° value is determined from the intercept to be 0.71 s^{-1}. Diffusion coefficient of 5-FU for the electrochemical

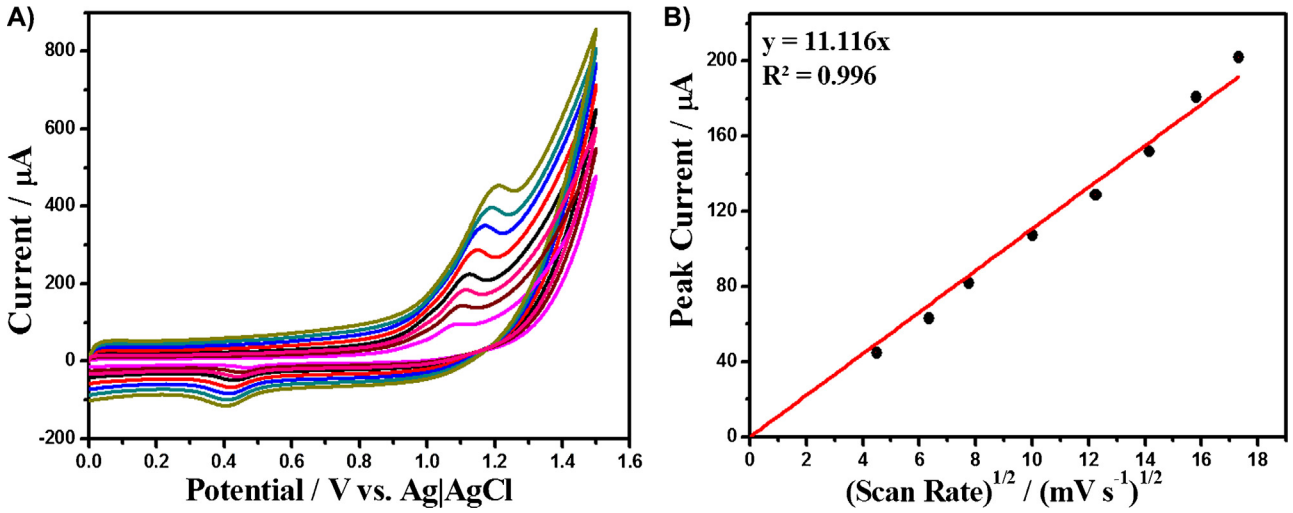

Fig. 5. (A) CVs of 0.5 mM 5-FU in B-R buffer (pH 8.0) recorded at GNP-MWCNT-Chit/GCE with different scan rates (20, 40, 60, 100, 150, 200, 250, 300, 350 mV s^{-1}). (B) Plot of the anodic peak current against the square root of scan rate.

oxidation at GNP-MWCNT-Chit/GCE is determined to be 2.93×10^{-5} cm^2 s^{-1}. Considering the results of Ep vs. pH studies together, we could conclude that the electrochemical oxidation of 5-FU is a one-electron one-proton transfer process, and these results are in well agreement with the mechanism for the oxidation of 5-FU proposed in previous reports (Scheme S1, Supplementary information) [7].

3.3. Electrochemical Impedance Spectroscopy (EIS)

Electrochemical impedance spectroscopy of the GNP nanocomposite electrode was examined to study the interfacial properties of the electrode and to examine the characteristics of the nanocomposite film. Charge transfer resistance (R_{ct}) determined here is an important characteristic of electron-transfer across the electrode interface [26,27]. Electrochemical impedance spectra of bare GCE, MWCNT-Chit/GCE, GNP-MWCNT-Chit/GCE in aq. 1 mM $K_3[Fe(CN)_6]$ + 0.1 M KCl were examined at the open circuit potential over the frequency range of 100 kHz to 10 mHz. The open circuit potential was approximately equal to the redox potential of $K_3[Fe(CN)_6]$ at its respective electrode. The results were analyzed with various equivalent circuit models, and the observed results were found to best fit with Randles equivalent circuit. The resulting Nyquist and Bode plots are shown in Fig. 6. The Nyquist plot of bare GCE shows a semi-circular pattern followed by a linear plot, and the charge-transfer resistance (R_{ct}) for electron-transfer at bare GCE is determined to be 2.3 kohm. However, the Nyquist plots of both MWCNT-Chit/GCE and GNP-MWCNT-Chit/GCE (Fig. 6(A)) exhibit only a linear plot relevant to a mere diffusion behavior alone, indicating the very good conductivity of the nanocomposite modified electrode with negligible charge transfer resistance. The Bode plots clearly show that the diffusion behavior of redox species towards the GNP-MWCNT-Chit/GCE was very high compared to MWCNT-Chit/GCE and that the active surface area was increased by decorating MWCNT with gold nanoparticles.

Both the cyclic voltammetry and EIS analysis results show that the GNP-MWCNT nanocomposite film provided a facile electron conduction pathway for catalyzed oxidation of 5-FU. That is to say, the GNP-MWCNT-Chit composite comprising long tubular conductive CNT coupled with gold nanoparticles and the fine dispersion of nanotubes in the chitosan matrix together made the electron transfer easier. The enhanced electron transfer could be ascribed to the nanolevel surface structural and morphological features of GNP and MWCNT, such as porous surface structure, continuous network of GNPs on MWCNT and excellent electrical conductivity of the GNP-MWCNT composite. The fabricated GNP-MWCNT-Chit/GCE is investigated for quantitative analysis of 5-FU.

3.4. Differential pulse voltammetry (DPV)

Differential pulse voltammetric analysis of 5-FU at the GNP nanocomposite electrode was carried out for quantitative analysis of 5-FU. Optimum experimental parameters for a good voltammetric profile with high peak current and minimal background current are established to be 100 mV pulse amplitude, 100 ms pulse width and 10 mV step increment. Differential pulse voltammograms of 5-FU at GNP-MWCNT-Chit/GCE electrode were recorded in B-R buffer (pH 8.0) over the concentration range of 0–10 μM 5-FU, and the results are shown in Fig. 7(A). A well defined anodic peak was observed at +0.95 V. The peak current increased gradually with the increase in the concentration of 5-FU. The DPV measurements were repeated four times with independent electrodes, and the peak current was plotted against the concentration of 5-FU. A linear plot with a regression coefficient of 0.99 was obtained, as shown in Fig. 7(B). Low-detection-limit of the sensor system is defined as the change in peak current by three relative standard deviations, and it is determined from the plot to be 20 nM. The linear determination range is 3×10^{-8}–10×10^{-6} M. The performance of the GNP nanocomposite electrode were compared with those reported previously [1,2,4,6–8,28–31], as shown in Table 1. The low-detection-limit of our study is very much comparable with those reported by various electrochemical methods, different modified electrodes and chromatographic and other analytical methods (Table 1). The performance of the present GNP nanocomposite electrode for the detection of 5-FU in the presence of various potential interferents and from complex physiological and pharmaceutical samples were further investigated.

3.5. Interferences

Electrochemical response of 5-FU in the presence of potentially electroactive biological compounds such as ascorbic acid (AA), uric acid (UA), dopamine (DA) and 5-hydroxytryptamine (5-HT) has been investigated at the GNP-MWCNT nanocomposite electrode by DPV method. Fig. 8 shows the DPVs at the GNP-MWCNT nanocomposite electrode in the mixture of AA, UA, DA and 5-HT 5 μM each and different concentrations of 5-FU at micromolar concentration levels (2, 4, 6, 8 μM) in B-R buffer (pH 8.0). At the GNP-MWCNT-Chit/GCE,

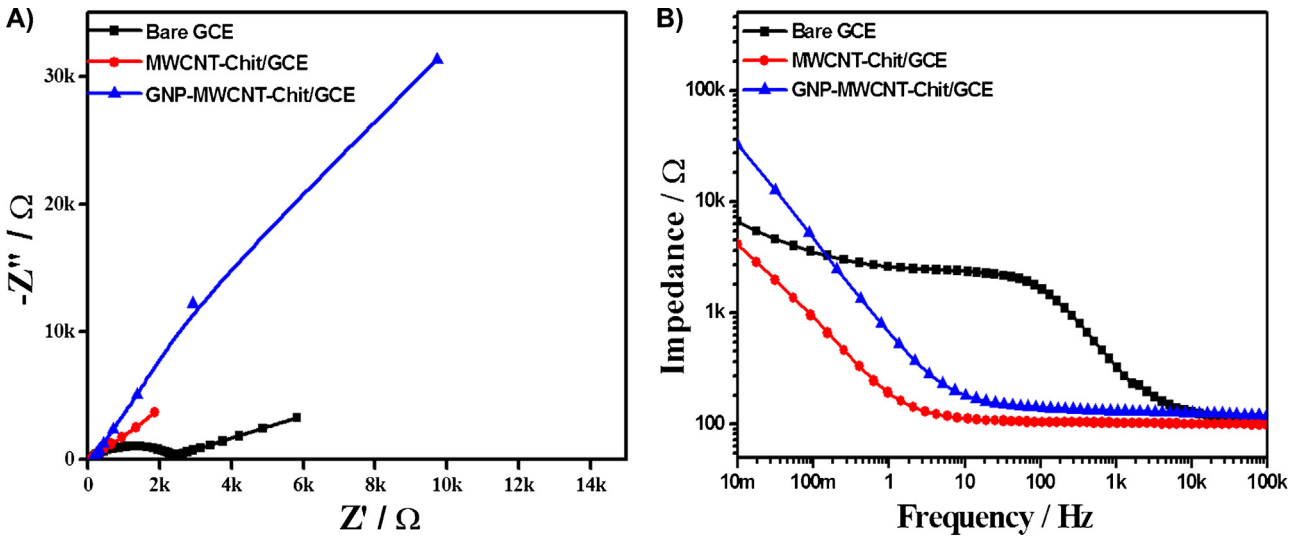

Fig. 6. (A) Nyquist and (B) Bode plots of EIS analysis at bare GCE, MWCNT-Chit/GCE and GNP-MWCNT-Chit/GCE in aq. 1 mM $K_3[Fe(CN)_6]$ + 0.1 M KCl.

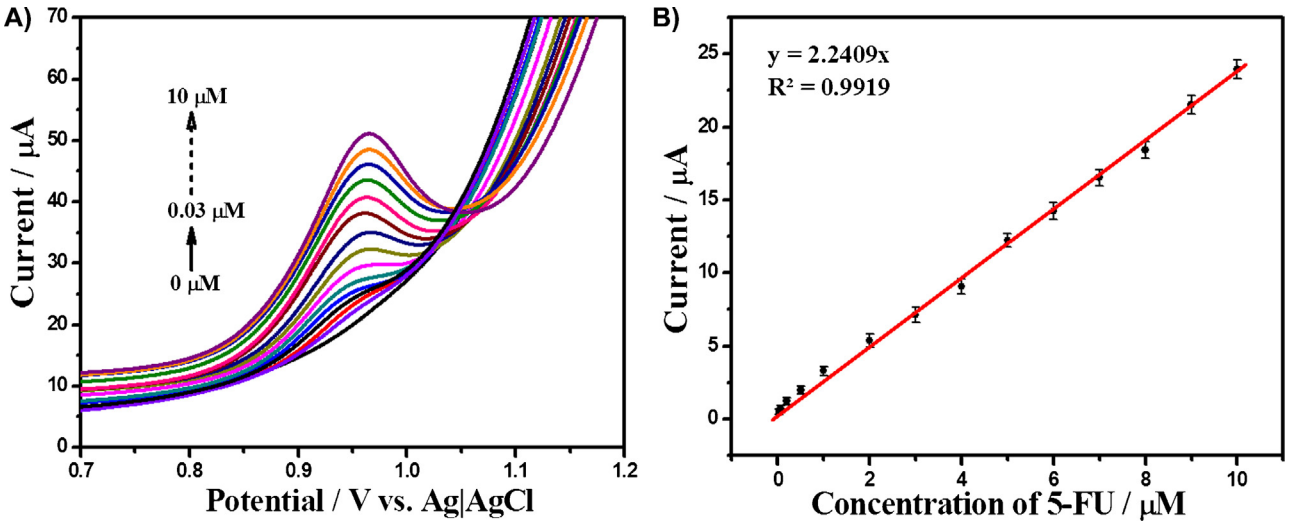

Fig. 7. (A) DPVs of 5-FU in B-R buffer (pH 8.0) at different concentrations (0, 0.03, 0.06, 0.2, 0.5, 1, 2, 3, 4, 5, 6, 7, 8, 9, 10 μM) at GNP-MWCNT-Chit/GCE. (B) Plot of i_p vs. 5-FU concentration.

Table 1
Detection of 5-FU using electrochemical and various analytical methods.

Method	Electrode	Linear range	Limit of detection	Reference
Potentiometry	Membrane electrode	1.3–130 μg mL $^{-1}$	10 μM	[30] Hassan et al. (1998)
Cyclic voltammetry	MWNT/BTB/GCE	0.8 μM–5 mM	0.26 μM	[6] Shen et al. (2013)
SWV	HMDE	10–90 pM	7.7 pM	[8] Mirceski et al. (2000)
SWV	AuNP-SPE	0.2–50 μg mL^{-1}	0.1 μg mL^{-1}	[31] Wang et al. (2012)
DPV	IL-CPE	0.5–800 μM	13 nM	[7] Hou et al. (2011)
DPASV	MIP-fiber electrode	9.9–426 ng mL $^{-1}$	1.30 ng mL $^{-1}$	[29] Prasad et al.(2012)
Vibrational Spectroscopy	n.a.	–	2 μg mL^{-1}	[1] Farquharson et al.(2005)
Spectrophotometry	n.a.	30–100 μg mL $^{-1}$	0.5 μg mL^{-1}	[2] Amer et al. (1997)
HPLC	n.a.	4–160 ng mL^{-1}	4 ng mL^{-1}	[4] Chu et al. (2003)
HPLC	n.a.	0.2–40 μg mL $^{-1}$	0.6 ng mL^{-1}	[28] Chen et al. (2012)
DPV	GNP-MWCNT-Chit/GCE	0.03–10 μM (3.9 ng mL^{-1}–1.3 μg mL^{-1})	2×10^{-8} M (2.6 ng mL^{-1})	Present work

BTB – Bromothymol blue, SWV – Square-wave voltammetry, HMDE – Hanging mercury drop electrode, AuNP-SPE – Gold nanoparticle-modified screen-printed electrode, DPASV – Differential pulse adsorptive stripping voltammetry, HPLC – High performance liquid chromatography, n.a. – Not applicable.

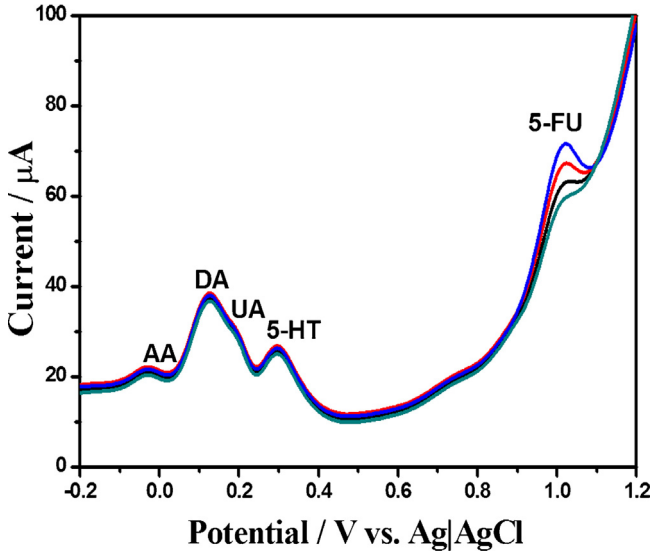

Fig. 8. DPVs recorded at GNP-MWCNT-Chit/GCE with 5-FU at different concentrations (2.0, 4.0, 6.0, 8.0) in the presence of AA, DA, UA and 5-HT 5 μM each in B-R buffer (pH 8.0).

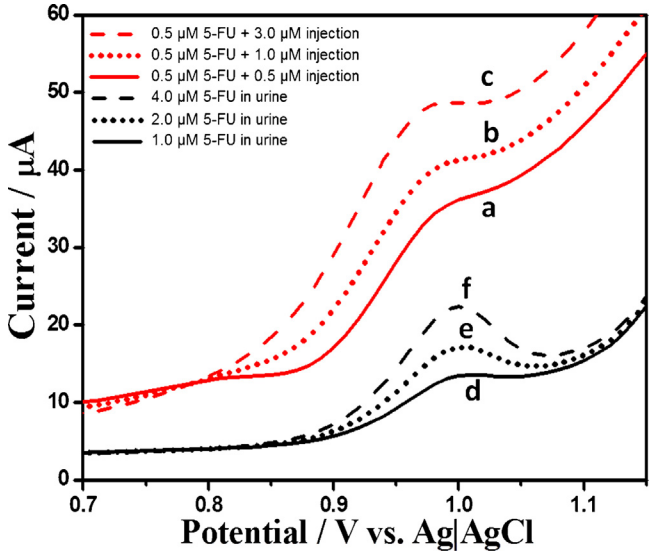

Fig. 9. DPVs recorded at GNP-MWCNT-Chit/GCE in the presence of a mixture of 0.5 μM pure 5-FU and different concentrations of 5-FU (a = 0.5 μM, b = 1.0 μM and c = 3.0 μM) from pharmaceutical formulation in B–R buffer (pH 8.0) and in the presence of (d = 1.0, e = 2.0 and f = 4.0 μM) 5-FU in artificial urine.

Table 2
Determination of 5-FU in pharmaceutical injection and in artificial urine samples using the GNP-MWCNT–Chit/GCE.

Sample	5-FU ($\times 10^{-6}$ M)	Injection Added ($\times 10^{-6}$ M)	[a]Found ($\times 10^{-6}$ M)	Average Recovery (%)	[a]RSD (%)
Injection (Fluracil, 250 mg/5 ml)	0.5	0.5	1.06	102.6	1.8
	0.5	1.5	2.05	100.7	1.3
	0.5	3.0	3.46	98.3	1.4
Urine Sample	1.0	–	0.98	98.9	0.9
	2.0	–	1.98	97.6	0.7
	4.0	–	4.02	101.4	1.2

[a] Mean value of six measurements.

distinct peaks for AA, DA, 5-HT and 5-FU each were observed with a merged peak of UA (Fig. 8). The peak currents for 5-FU increased as the concentration of 5-FU increases in the presence of these interferences. Even higher concentrations of AA, DA, UA and 5-HT together could not affect the current response of 5-FU in B-R buffer. From the experimental results, it is clearly evident that the proposed electrochemical sensor can be used effectively for the detection of 5-FU even in the presence of various possible electroactive interferents.

3.6. Reproducibility and Reusability

The stability, reusability and reproducibility of the GNP nanocomposite electrodes for the detection of 5-FU was investigated by DPV analysis. DPVs of 20 μM 5-FU were recorded at a single GNP-MWCNT-Chit/GCE electrode over a period of 7 days, while storing the modified electrode at ambient laboratory conditions. The peak currents of the recorded DPVs decreased merely by 3.8% in about 25 measurements, and this observation clearly indicates the stability and reusability of the fabricated GNP nanocomposite electrode. Further, reproducibility of the modified electrode was examined by recording DPVs of 5-FU in multiple measurements with the use of six GNP-MWCNT-Chit/GCE electrodes fabricated independently. The peak currents of the DPVs of 20 μM 5-FU recorded at these electrodes varied to an extent of only 2.4%. It clearly reveals that the nanocomposite electrode is highly reproducible for the analysis of 5-FU. In overall, all the observations conclude that the reusability and reproducibility of the GNP nanocomposite electrode are quite satisfactory.

3.7. Determination of 5-FU in pharmaceutical and artificial urine samples

Pharmaceutical samples of 5-FU (Fluracil 250 mg/5 mL injection) were analyzed by using the fabricated nanocomposite sensor with the standard addition method. In Fig. 9, curves "a, b and c" show the DPVs of the analytical samples containing 0.5 μM of pure 5-FU together with different concentrations (0.5, 1 and 3 μM) of 5-FU of the pharmaceutical injection at the GNP-MWCNT-Chit/GCE. The experimental time for a DPV analysis is as low as 25 s. The recovery values obtained in these experiments varied from 98.3% to 102.6% (Table 2) and are quite satisfactory. Recovery of 5-FU from artificial urine was examined by the addition of 5-FU into undiluted artificial urine of pH 8.0 without any buffer. In Fig. 9, curves "d, e and f" show the DPVs of the GNP-MWCNT-Chit/GCE electrode recorded in the artificial urine sample in the presence of 1.0, 2.0 and 4.0 μM 5-FU. The recovery of 5-FU from undiluted artificial urine samples at different concentrations of 5-FU (1.0–4.0 μM) varied from 97.6% to 101.4% (Table 2). In physiological samples of clinical patients, the mean concentration of 5-FU varies over a wide concentration range of 0.106–3.77 μg mL^{-1} (0.82–29.2 μM) in serum samples [32,33] and as high as 10–60 μg mL^{-1} (77.4–464.2 μM) in urine samples [3,34]. The linear determination range of the developed sensor (0.03–10 μM) along with the very good recovery limits for physiological urine and pharmaceutical samples clearly confirms that the developed nanocomposite sensor would be of biomedical interest.

4. Conclusions

In this work, we synthesized chitosan biopolymer protected GNPs and decorated on the surface of MWCNT with an effective linkage between them. Further, a stable and efficient electrochemical biosensor based on GNP-MWCNT nanocomposite electrode was fabricated for sensitive determination of 5-FU by simple drop-cast method. The GNP-MWCNT nanocomposite film remarkably enhanced the current response and decreased the oxidation overpotential of 5-FU. In the GNP nanocomposite modified electrode, both fine dispersion of MWCNT in the nanocomposite film and the continuous network of GNPs of finite size (~28.7 nm) on the CNT chain helped for a facile electron-transfer across the film and for a good electrocatalytic activity. The present electrochemical biosensor was efficient for the detection of ppb levels (ng mL^{-1}) of 5-FU despite the presence of potential electroactive interferents and had shown good recovery limits for direct determination from biological fluids and pharmaceutical formulations with the analysis time of as low as 25 s. The fabricated biosensor exhibited good stability, high sensitivity and simple fabrication procedure. All the advantages obtained with the present biosensor system confirm that the nanocomposite based biosensor coupling CNT, nanometallic particle and a green biopolymer chitosan could be explored and extended for selective determination of various pharmaceutical drugs.

Acknowledgements

The authors gratefully acknowledge the Ministry of Human Resource Development, India and the National Institute of Technology, Warangal for Junior Research Fellowship to MS and for financial support.

This work is dedicated to Professor R. Ramaraj on his 60th Birthday for his pioneering research in the fields of Photochemistry and Electrochemistry.

Appendix A. Supplementary data

Supplementary data associated with this article can be found, in the online version, at http://dx.doi.org/10.1016/j.electacta.2015.08.036.

References

[1] S. Farquharson, A.D. Gift, C. Shende, P. Maksymiuk, F.E. Inscore, J. Murran, Detection of 5-fluorouracil in saliva using surface-enhanced Raman spectroscopy, Vib. Spectrosc. (2005) 79–84, doi:http://dx.doi.org/10.1016/j.vibspec.2005.02.021.

[2] M.M. Amer, S.S. Hassan, S.A. Abd El-Fatah, A.M. El-Kosasy, Spectrophotometric and spectrofluorimetric determination of fluorouracil in the presence of its degradation products, J. Pharm. Pharmacol. 50 (1998) 133–138, doi:http://dx.doi.org/10.1111/j.2042-7158.1998.tb06167.x.
[3] M. Barberi-Heyob, J.L. Merlin, B. Weber, Analysis of 5-fluorouracil in plasma and urine by high-performance liquid chromatography, J. Chromatogr. B Biomed. Sci. Appl 581 (1992) 281–286, doi:http://dx.doi.org/10.1016/0378-4347(92)80.283-V.
[4] D. Chu, J. Gu, W. Liu, J.P. Fawcett, Q. Dong, Sensitive liquid chromatographic assay for the simultaneous determination of 5-fluorouracil and its prodrug, tegafur, in beagle dog plasma, J. Chromatogr. B Anal. Technol. Biomed. Life Sci. 795 (2003) 377–382, doi:http://dx.doi.org/10.1016/S1570-0232(03)571-3.
[5] A. Procházková, S. Liu, H. Friess, S. Aebi, W. Thormann, Determination of 5-fluorouracil and 5-fluoro-2′-deoxyuridine-5'-monophosphate in pancreatic cancer cell line and other biological materials using capillary electrophoresis, J. Chromatogr. A 916 (2001) 215–224, doi:http://dx.doi.org/10.1016/S0021-9673(00)1171-7.
[6] X. Hua, X. Hou, X. Gong, G. Shen, Electrochemical behavior of 5-fluorouracil on a glassy carbon electrode modified with bromothymol blue and multi-walled carbon nanotubes, Anal. Methods 5 (2013) 2470, doi:http://dx.doi.org/10.1039/c3ay40149a.
[7] T. Zhan, L. Cao, W. Sun, W. Hou, Electrochemical behavior of 5-fluoro-1H-pyrimidine-2 on an ionic liquid modified carbon paste electrode, Anal. Methods 3 (2011) 2651, doi:http://dx.doi.org/10.1039/c1ay05454f.
[8] V. Mirčeski, R. Gulaboski, B. Jordanoski, Š. Komorsky-Lovrić, Square-wave voltammetry of 5-fluorouracil, J. Electroanal. Chem. 490 (2000) 37–47, doi:http://dx.doi.org/10.1016/S0022-0728(00)203-5.
[9] G.A. Rivas, M.D. Rubianes, M.C. Rodríguez, N.F. Ferreyra, G.L. Luque, M.L. Pedano, et al., Carbon nanotubes for electrochemical biosensing, Talanta 74 (2007) 291–307, doi:http://dx.doi.org/10.1016/j.talanta.2007.10.013.
[10] L. Agüí, P. Yáñez-Sedeño, J.M. Pingarrón, Role of carbon nanotubes in electroanalytical chemistry: a review, Anal. Chim. Acta 622 (2008) 11–47, doi:http://dx.doi.org/10.1016/j.aca.2008.05.070.
[11] M.E. Ghica, R. Pauliukaite, O. Fatibello-Filho, C.M.A. Brett, Application of functionalised carbon nanotubes immobilised into chitosan films in amperometric enzyme biosensors, Sensors Actuators B Chem 142 (2009) 308–315, doi:http://dx.doi.org/10.1016/j.snb.2009.08.012.
[12] S. Murugesan, K. Myers, V, (Ravi) Subramanian, Amino-functionalized and acid treated multi-walled carbon nanotubes as supports for electrochemical oxidation of formic acid, Appl. Catal. B Environ 103 (2011) 266–274, doi:http://dx.doi.org/10.1016/j.apcatb.2010.07.038.
[13] R.K. Gupta, M.P. Srinivasan, R. Dharmarajan, Synthesis of 16-Mercaptohexadecanoic acid capped gold nanoparticles and their immobilization on a substrate, Mater. Lett. 67 (2012) 315–319, doi:http://dx.doi.org/10.1016/j.matlet.2011.09.047.
[14] S.S. Nair, S.A. John, T. Sagara, Simultaneous determination of paracetamol and ascorbic acid using tetraoctylammonium bromide capped gold nanoparticles immobilized on 1,6-hexanedithiol modified Au electrode, Electrochim. Acta 54 (2009) 6837–6843, doi:http://dx.doi.org/10.1016/j.electacta.2009.06.077.
[15] P. Kannan, S.A. John, Fabrication of conducting polymer-gold nanoparticles film on electrodes using monolayer protected gold nanoparticles and its electrocatalytic application, Electrochim. Acta 56 (2011) 7029–7037, doi:http://dx.doi.org/10.1016/j.electacta.2011.06.004.
[16] M. Satyanarayana, K.K. Reddy, K.V. Gobi, Multiwall carbon nanotube ensembled biopolymer electrode for selective determination of isoniazid in vitro, Anal. Methods 6 (2014) 3772–3778, doi:http://dx.doi.org/10.1039/c4ay00154k.
[17] C.W. Brooks, A simple artificial urine for the growth of urinary pathogens, Lett. Appl. Microbiol. 24 (1997) 203–206, doi:http://dx.doi.org/10.1046/j.1472-765X.1997.00378.x.
[18] C. Gouveia-Caridade, R. Pauliukaite, C.M.A. Brett, Development of electrochemical oxidase biosensors based on carbon nanotube-modified carbon film electrodes for glucose and ethanol, Electrochim. Acta 53 (2008) 6732–6739, doi:http://dx.doi.org/10.1016/j.electacta.2008.01.040.
[19] H. Huang, X. Yang, Synthesis of chitosan-stabilized gold nanoparticles in the absence/presence of tripolyphosphate, Biomacromolecules 5 (2004) 2340–2346, doi:http://dx.doi.org/10.1021/bm0497116.
[20] N.R. Jana, L. Gearheart, C.J. Murphy, Seeding growth for size control of 5-40 nm diameter gold nanoparticles, Langmuir 17 (2001) 6782–6786, doi:http://dx.doi.org/10.1021/la0104323.
[21] D. Ghosh, Gold Nanoparticles: Acceptors for Efficient Energy Transfer from the Photoexcited Fluorophores, Opt. Photonics J. 03 (2013) 18–26, doi:http://dx.doi.org/10.4236/opj.2013.31004.
[22] H. Sharma, D.C. Agarwal, a, K. Shukla, D.K. Avasthi, V.D. Vankar, Surface-enhanced Raman scattering and fluorescence emission of gold nanoparticle-multiwalled carbon nanotube hybrids, J. Raman Spectrosc. 44 (2013) 12–20, doi:http://dx.doi.org/10.1002/jrs.4136.
[23] D.N. Travessa, F.S. da Silva, F.H. Cristovan, A.M. Jorge Jr, K.R. Cardoso, Ag ion decoration for surface modifications of multi-walled carbon nanotubes, Mater. Res 17 (2014) 687–693, doi:http://dx.doi.org/10.1590/S1516-14392014005000026.
[24] S. Hrapovic, E. Majid, Y. Liu, K. Male, J.H.T. Luong, Metallic nanoparticle-carbon nanotube composites for electrochemical determination of explosive nitroaromatic compounds, Anal. Chem. 78 (2006) 5504–5512, doi:http://dx.doi.org/10.1021/ac060435q.
[25] E. Laviron, General expression of the linear potential sweep voltammogram in the case of diffusionless electrochemical systems, J. Electroanal. Chem 101 (1979) 19–28.
[26] Y. Feng, T. Yang, W. Zhang, C. Jiang, K. Jiao, Enhanced sensitivity for deoxyribonucleic acid electrochemical impedance sensor: gold nanoparticle/polyaniline nanotube membranes, Anal. Chim. Acta 616 (2008) 144–151, doi:http://dx.doi.org/10.1016/j.aca.2008.04.022.
[27] R. Pauliukaite, M.E. Ghica, O. Fatibello-Filho, C.M.A. Brett, Electrochemical impedance studies of chitosan-modified electrodes for application in electrochemical sensors and biosensors, Electrochim. Acta 55 (2010) 6239–6247, doi:http://dx.doi.org/10.1016/j.electacta.2009.09.055.
[28] W. Chen, Y. Shen, H. Rong, L. Lei, S. Guo, Development and application of a validated gradient elution HPLC method for simultaneous determination of 5-fluorouracil and paclitaxel in dissolution samples of 5-fluorouracil/paclitaxel-co-eluting stents, J. Pharm. Biomed. Anal 59 (2012) 179–183, doi:http://dx.doi.org/10.1016/j.jpba.2011.10.005.
[29] B.B. Prasad, D. Kumar, R. Madhuri, M.P. Tiwari, Nonhydrolytic sol-gel derived imprinted polymer-multiwalled carbon nanotubes composite fiber sensors for electrochemical sensing of uracil and 5-fluorouracil, Electrochim. Acta 71 (2012) 106–115, doi:http://dx.doi.org/10.1016/j.electacta.2012.03.110.
[30] S.S. Hassan, M.M. Amer, S.A. Abd El-Fatah, A.M. El-Kosasy, Membrane sensors for the selective determination of fluorouracil, Anal. Chim. Acta 363 (1998) 81–87, doi:http://dx.doi.org/10.1016/S0003-2670(98)62-2.
[31] S. Wang, S. Fu, H. Ding, Determination of 5-Fluorouracil Using Disposable Gold Nanoparticles Modified Screen-Printed Electrode, Sens. Lett 10 (2012) 974–978, doi:http://dx.doi.org/10.1166/sl.2012.2341.
[32] G. Bocci, R. Danesi, A. Di Paolo, F. Innocenti, G. Allegrini, A. Falcone, et al., Comparative Pharmacokinetic Analysis of 5-Fluorouracil and Its Major Metabolite 5-Fluoro-5, 6-dihydrouracil after Conventional and Reduced Test Dose in Cancer Patients 1, Clin. Cancer Res. 6 (2000) 3032–3037.
[33] T. Yoshida, E. Araki, M. Iigo, T. Fujiil, M. Yoshino, Y. Shimadal, ancer hemotherapyand harmacology, et al., Clinical significance of monitoring serum levels of 5-fluorouracil by continuous infusion in patients with advanced colonic cancer, Cancer Chemother Pharmacol 26 (1990) 352–354.
[34] W.E. Hull, E. Port, R. Herrmann, W. Kunz, Metabolites of 5-Fluorouracil in plasma and urineas Monitored by ^{19}F Nuclear Magnetic Resonance Spectroscopy, for Patients Receiving Chemotherappy with or without Methotrexate Pretreatment, Cancer Res. 48 (1988) 1680–1688.